AGU PUBLICATIONS

Geochemistry, Geophysics, Geosystems

RESEARCH ARTICLE
10.1002/2015GC005844

A Bayesian, multivariate calibration for *Globigerinoides ruber* Mg/Ca

D. Khider[1,2], G. Huerta[3], C. Jackson[1], L. D. Stott[2], and J. Emile-Geay[2]

[1]Institute for Geophysics, University of Texas at Austin, Austin, Texas, USA, [2]Department of Earth Science, University of Southern California, Los Angeles, California, USA, [3]Department of Mathematics and Statistics, University of New Mexico, Albuquerque, New Mexico

Key Points:
- New Bayesian calibration for *G. ruber* Mg/Ca
- Multivariate model accounts for temperature, salinity, and dissolution
- Secondary influences on *G. ruber* Mg/Ca are a large source of systematic error

Supporting Information:
- Supporting Information S1
- Table S1
- Table S2
- Software S1
- Software S2

Correspondence to:
D. Khider,
khider@usc.edu

Citation:
Khider, D., G. Huerta, C. Jackson, L. D. Stott, and J. Emile-Geay (2015), A Bayesian, multivariate calibration for *Globigerinoides ruber* Mg/Ca, *Geochem. Geophys. Geosyst.*, *16*, 2916–2932, doi:10.1002/2015GC005844.

Received 3 APR 2015
Accepted 18 JUL 2015
Accepted article online 22 JUL 2015
Published online 6 SEP 2015

Abstract The use of Mg/Ca in marine carbonates as a paleothermometer has been challenged by observations that implicate salinity as a contributing influence on Mg incorporation into biotic calcite and that dissolution at the sea-floor alters the original Mg/Ca. Yet, these factors have not yet been incorporated into a single calibration model. We introduce a new Bayesian calibration for *Globigerinoides ruber* Mg/Ca based on 186 globally distributed core top samples, which explicitly takes into account the effect of temperature, salinity, and dissolution on this proxy. Our reported temperature, salinity, and dissolution (here expressed as deep-water ΔCO_3^{2-}) sensitivities are ($\pm 2\sigma$) 8.7±0.9%/°C, 3.9±1.2%/psu, and 3.3±1.3%/μmol.kg^{-1} below a critical threshold of 21 μmol/kg in good agreement with previous culturing and core-top studies. We then perform a sensitivity experiment on a published record from the western tropical Pacific to investigate the bias introduced by these secondary influences on the interpretation of past temperature variability. This experiment highlights the potential for misinterpretations of past oceanographic changes when the secondary influences of salinity and dissolution are not accounted for. Multiproxy approaches could potentially help deconvolve the contributing influences but this awaits better characterization of the spatio-temporal relationship between salinity and $\delta^{18}O_{sw}$ over millennial and orbital timescales.

1. Introduction

Mg/Ca paleothermometry is one of the most common techniques used to reconstruct sea surface temperature (SST) conditions [e.g., *Anand et al.*, 2003; *Dekens et al.*, 2002; *Lea et al.*, 1999; *Nürnberg et al.*, 1996]. Thermodynamic and calibration studies have shown that an empirical regression of Mg/Ca versus temperature is exponential and the temperature sensitivity is close to 9%/°C for surface-dwelling planktonic foraminifera [e.g., *Anand et al.*, 2003]. Furthermore, when used in conjunction with measurements of the stable oxygen isotope composition ($\delta^{18}O_c$) from the same foraminiferal sample, it is potentially possible to deconvolve the temperature, local salinity (i.e., local $\delta^{18}O_{sw}$) and, on long time scales, global ice volume influences on calcite $\delta^{18}O$ [e.g., *Elderfield and Ganssen*, 2000; *Lea et al.*, 2000; *Stott et al.*, 2002]. To do so, however, requires the assumption that temperature is the dominant control on Mg incorporation into foraminiferal calcite.

Earlier studies have recognized that Mg incorporation in foraminiferal tests can be affected by other localized influences such as pressure [*Elderfield et al.*, 1996], carbonate dissolution [*Barker et al.*, 2005; *Brown and Elderfield*, 1996; *de Villiers*, 2003; *Dekens et al.*, 2002; *Nouet and Bassinot*, 2007; *Regenberg et al.*, 2006, 2014; *Rosenthal and Lohmann*, 2002], carbonate ion concentration [*Kisakürek et al.*, 2008; *Russell et al.*, 2004], shell size [*Elderfield et al.*, 2002; *Friedrich et al.*, 2012], as well as salinity [*Arbuszewski et al.*, 2010; *Dueñas-Bohorquez et al.*, 2009; *Hönisch et al.*, 2013; *Kisakürek et al.*, 2008; *Lea et al.*, 1999; *Mathien-Blard and Bassinot*, 2009; *Nürnberg et al.*, 1996; *Sadekov et al.*, 2009]. Carbonate dissolution is a well-documented influence on the Mg/Ca of biogenic calcite. Dissolution within the water column, at the sediment-water interface, and also within the sediments, can occur when the in situ carbonate ion concentration ($[CO_3^{2-}]_{obs}$) is lower than the saturation concentration ($[CO_3^{2-}]_{sat}$, and $\Delta CO_3^{2-} = [CO_3^{2-}]_{obs} - [CO_3^{2-}]_{sat} < 0$) [*Berger et al.*, 1982] and this will result in a preferential removal of Mg-rich calcite from the foraminiferal test and thus a cold-temperature bias for the proxy [*Barker et al.*, 2005; *Dekens et al.*, 2002; *Fehrenbacher and Martin*, 2014; *Regenberg et al.*, 2006].

In addition to dissolution, culturing [*Hönisch et al.*, 2013; *Kisakürek et al.*, 2008; *Lea et al.*, 1999] and core-top [*Arbuszewski et al.*, 2010; *Mathien-Blard and Bassinot*, 2009; *Sadekov et al.*, 2009] studies have found a salinity

influence on *G. ruber* Mg/Ca, evidenced by the presence of "excess Mg/Ca" or "excess temperature" that would otherwise be predicted from existing Mg/Ca-temperature relationships.

In this study, we will consider these two secondary influences to develop a comprehensive calibration model for *G. ruber* thermometry based on Bayesian inference. Our aims are to (1) estimate the probability distributions of Mg/Ca sensitivity to SST, sea surface salinity (SSS) and deep-water ΔCO_3^{2-}, used here as a proxy for dissolution, from a combined database of 186 core-top samples with a global geographical coverage (section 3), and to (2) evaluate the magnitude of the systematic error introduced by ignoring secondary effects on *G. ruber* Mg/Ca (section 5) using a published Mg/Ca record from the Indonesian Seas (core MD98–2181 (MD81), 6.3°N, 125.82°E, 2114 m water depth [*Stott et al*., 2007]). The purpose here is not to rewrite the deglacial history of the Indo-Pacific Warm Pool based on a single sedimentary record but rather discuss how best to report the uncertainties associated with SST reconstructions and their potential implications for model-data comparisons.

2. Methods

2.1. Bayesian Inference

Bayesian inference provides several advantages for the calibration exercises over the more-traditional frequentist approach since it allows one to directly propagate the uncertainty in the calibration model into an uncertainty in the predictions of environmental parameters [*Tierney and Tingley*, 2014]. It can handle complex models with many parameters [*Gelman et al*., 2013]. Bayesian inference has been applied to several problems in climate research [e.g., *Berliner et al*., 2000a, 2000b; *Blaauw and Christen*, 2011; *Haslett and Parnell*, 2008; *Haslett et al*., 2006; *Jackson et al*., 2008; *Lin et al*., 2014; *Parnell et al*., 2014; *Tebaldi et al*., 2005; *Tingley and Huybers*, 2010], including the calibration of the TEX86 paleothermometer [*Tierney and Tingley*, 2014]. Bayesian statistics proceeds by drawing a set of samples from a prior probability distribution and updating the probability of these parameters in light of new data. The characteristics of the prior distribution are determined by information available before the new data have been analyzed and reflect previous scientific understanding and/or the analyst's subjective judgment about the parameters. Bayes' theorem then combines the prior density distribution and the new data in the posterior probability distribution of the parameter, which measures how plausible the prior value of the parameter is once we have observed the data:

$$\pi(unknowns \mid data) \propto f(data \mid unknowns) \cdot \pi(unknowns) \quad (1)$$

The term $\pi(unknowns|data)$ represents the probability of the unknown given the data and is called the posterior distribution; $f(data|unknowns)$ is the likelihood of the data given the unknowns; and $\pi(unknowns)$ are the prior probability distributions on the unknowns. For the calibration model presented in this study, the unknowns represent the sensitivity coefficients and the variance on the Mg/Ca data, τ^2. In this study, we used the JAGS software package for Bayesian inference using the Gibbs sampler (http://mcmc-jags.sourceforge.net). The Gibbs sampler proceeds numerically, via Markov Chain Monte Carlo (MCMC) simulations. The basic idea behind this algorithm is to sample full conditional distributions based on proposed distributions to generate sets of coefficients that are linked in a Markov Chain (i.e., each sample is only directly related to the previous one) and a criterion for rejecting or accepting the proposed moves.

2.2. Hydrographic Conditions

Our new calibration for *G. ruber* Mg/Ca is based on a compiled database of 186 core-top samples. The core-top data sets of *Mathien-Blard and Bassinot* [2009] (n = 24), *Arbuszewski et al*. [2010] (n = 32), *Dekens et al*. [2002] (n = 11), *Xu et al*. [2010] (n = 18), *Farmer* [2005] (n = 4), *Sabbatini et al*. [2011] (n = 17), and *Mohtadi et al*. [2011] (n = 59) were merged with additional measurements on 21 core tops with a global geographical coverage (Figure 1). This combination of data sets gathers sites spanning a comprehensive range of SST and SSS within which *G. ruber* calcifies, and deep-water ΔCO_3^{2-}, where fossil specimens accumulate on the seafloor. Because of the potential dissolution bias in the tropical Atlantic [*Hertzberg and Schmidt*, 2013], we omitted the data from this region. Mean annual and warm-season temperature and salinity data at each core top location were extracted from the World Ocean Atlas 13 (WOA13) [*Locarnini et al*., 2013; *Zweng et al*., 2013]. Following *Hertzberg and Schmidt* [2013] and *Hönisch et al*. [2013], we used mean annual temperature in the tropics (23°S-23°N) and warm-season temperature in the subtropics for the calibration. We

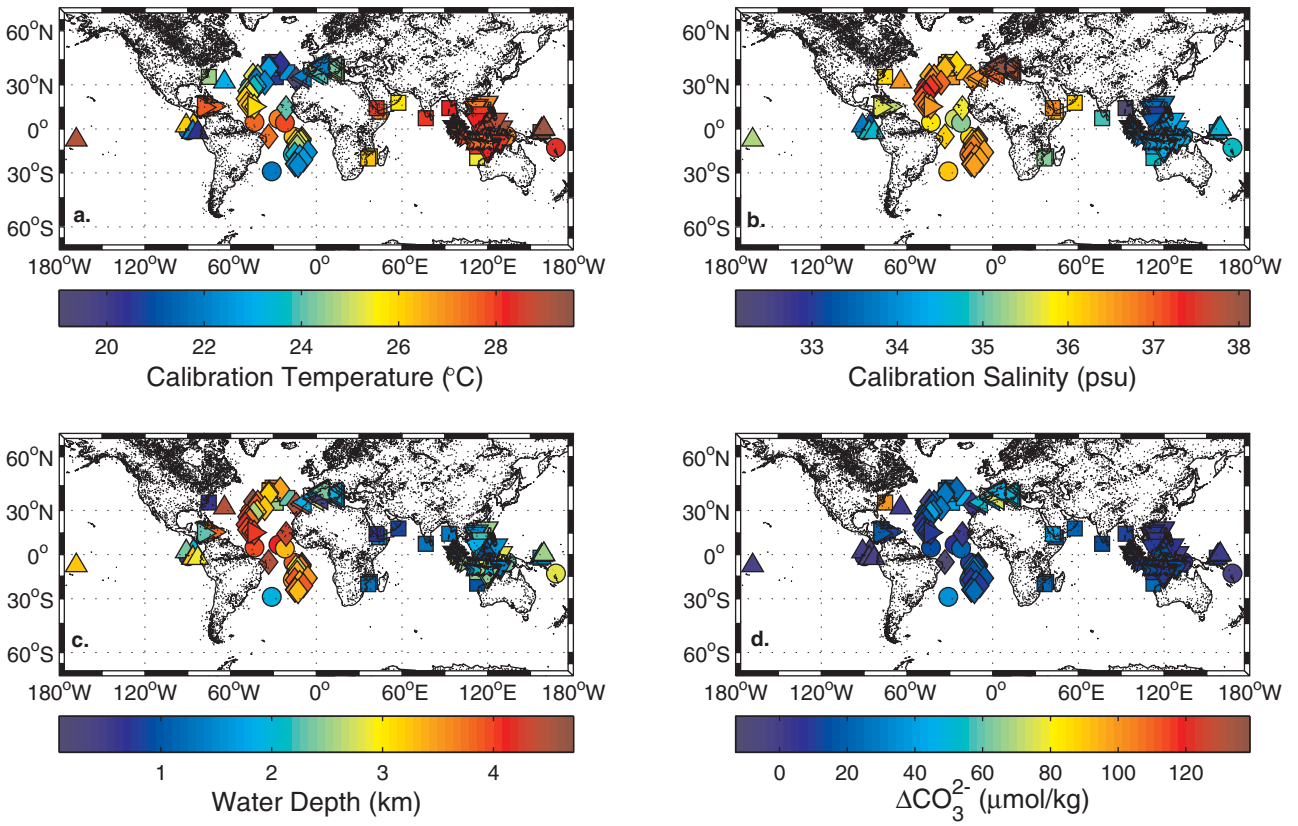

Figure 1. Sample Location. Circle: This study; Square: *Mathien-Blard and Bassinot* [2009]; Diamond: *Arbuszewski et al.* [2010]; Upward-pointing triangle: *Dekens et al.* [2002]; Downward-pointing triangle: *Xu et al.* [2010]; Right-pointing triangle: *Farmer* [2005]; Left-pointing triangle: *Sabbatini et al.* [2011]; Star: *Mohtadi et al.* [2011]. The filled colors represent: (a) Calibration temperature inferred from the World Ocean Atlas 13 [*Locarnini et al.*, 2013]. (b) Mean Calibration salinity inferred from the World Ocean Atlas 13 [*Zweng et al.*, 2013]. (c) Water depth (km), and (d) Estimated deep-water ΔCO_3^{2-} at the core locations.

also used a slightly deeper habitat depth (0–30 m) in the tropics than in the subtropics (0–15 m) [*Hönisch et al.*, 2013; *Mohtadi et al.*, 2009; *Sabbatini et al.*, 2011].

Since we are investigating the effect of carbonate dissolution on foraminiferal Mg/Ca, we estimated the departure from deep-water calcite saturation ΔCO_3^{2-} at each site based on the gridded alkalinity and total dissolved inorganic carbon data from the GLODAP database [*Key et al.*, 2004], and temperature, salinity, phosphate and silicate from the World Ocean Atlas 09 [*Antonov et al.*, 2010; *Garcia et al.*, 2010; *Locarnini et al.*, 2010] using the Program Developed for CO_2 Calculations adapted for the Matlab software [*van Hueven et al.*, 2009]. For the Mediterranean Sea, we used bottom alkalinity and pH data from the MEDAR database. For the Indonesian Seas, we used the ΔCO_3^{2-} at the effective sill depth. The hydrographic parameters are summarized in supporting information Table S1.

2.3. Analytical Techniques

Holocene age control on the core top samples analyzed in this study was confirmed by either radiometric dating or stable isotope stratigraphy. We assumed that WOA13 instrumental measurements of temperature, salinity, and deep-water ΔCO_3^{2-} are representative of the Holocene. However this is not strictly true, especially looking at the magnitude of Holocene millennial-scale variability at the core locations [e.g., *Debret et al.*, 2007; *Jansen et al.*, 2007; *Laepple and Huybers*, 2013] as well as the changes that have occurred over the 20th century. Thus the assumption that measured Mg/Ca reflects the modern conditions within the WOA13 data set introduces an additional source of independent errors in the interpretation of the Mg/Ca data, which we take into consideration through our τ^2 parameter (section 3).

For the present study, additional *G. ruber* Mg/Ca results have been added from the core top bulk sediment samples that were disaggregated in a sodium hexametaphosphate solution and wet-sieved over a 63 μm mesh to remove the clay fraction. This >63 μm fraction was then dry-sieved for the 250–350 μm fraction in

order to minimize possible size effects on the incorporation of Mg in the calcite lattice [*Elderfield et al*., 2002; *Friedrich et al*., 2012; *Richey et al*., 2012]. Approximately 150–200 specimens of *G. ruber* (white, sensu stricto and sensu lato, supporting information Text S1) from each sample were picked under a binocular microscope. The foraminifera were then gently cracked open between two glass plates in order to expose the chambers for cleaning and cleaned according to the *Barker et al*. [2003] protocol (hereafter referred to as BCP).

This cleaning technique was also used by *Mathien-Blard and Bassinot* [2009], *Sabbatini et al*. [2011], and *Mohtadi et al*. [2011]. On the other hand, *Arbuszewski et al*. [2010], *Dekens et al*. [2002], *Farmer* [2005], and *Xu et al*. [2010] used a fully reductive cleaning protocol. Laboratory experiments have shown that tests cleaned using the reductive technique tend to have Mg/Ca values 6–15% lower than those cleaned using the BCP [*Arbuszewski et al*., 2010; *Rosenthal et al*., 2004; *Xu et al*., 2010]. *Rosenthal et al*. [2004] also found that data generated with either of these methods are within analytical errors of each other, suggesting that variations among different data sets using the same cleaning methodologies only reflect analytical uncertainty. We take this difference in cleaning methodologies into account in the Bayesian analysis by prescribing a "cleaning offset" to the reductively cleaned data sets.

For Mg/Ca analysis, the foraminiferal samples were dissolved in 500 μL of 5% nitric acid solution and analyzed on a Jobin Yvon ICP-AES housed at the University of Southern California. Each sample measurement was bracketed by a standard solution made from solid Mg and reagent grade $CaCO_3$ in an elemental ratio of 5.63 mmol/mol, used to adjust the foraminiferal sample Mg/Ca for instrument drift. The average precision on the foraminiferal sample replicates is $1\sigma = \pm 0.2$ mmol/mol. Fe/Ca and Mn/Ca ratios were used to monitor potential contamination. The Mg/Ca values are summarized in supporting information Table S1.

3. Calibration Model

Unlike the TEX86 model, which uses an implicit spatially varying model to take into consideration ecological and sedimentary factors that are poorly understood [*Tierney and Tingley*, 2014], we employ an explicit model that takes into consideration the main controls on Mg/Ca. The underlying assumption in our model is that the Mg/Ca sensitivities to temperature, salinity, and dissolution as well as analytical biases are well understood and have been quantified separately in culturing, sediment-trap, and core-top studies. Here, we use these previous results to set the functional form of the Mg/Ca calibration model and to set the priors on the sensitivity coefficients (section 3.1).

To take into account the threshold effect of dissolution on foraminiferal Mg/Ca [*Regenberg et al*., 2014], we consider the following piecewise nonlinear regression model to describe the sensitivity of Mg/Ca to temperature T (α_1), salinity S (α_2), and deep-water ΔCO_3^{2-} (α_3):

$$\begin{gathered}
\text{if } \Delta CO_{3\,(i)}^{2-} \geq 21\mu mol/kg,\ \ Mg/Ca_{(i)} = \left(\exp\left(\alpha_1 T_{(i)} + \alpha_2 S_{(i)} + \alpha_0\right) + \alpha_3 21\right)/\left(1 + \alpha_4 C_{(i)}\right) + \varepsilon_{(i)} \\
\text{if } \Delta CO_{3\,(i)}^{2-} < 21\mu mol/kg,\ \ Mg/Ca_{(i)} = \left(\exp\left(\alpha_1 T_{(i)} + \alpha_2 S_{(i)} + \alpha_0\right) + \alpha_3 \Delta CO_{3\,(i)}^{2-}\right)/\left(1 + \alpha_4 C_{(i)}\right) + \varepsilon_{(i)} \\
\varepsilon_{(i)} \sim N(0, \tau^2)
\end{gathered} \tag{2}$$

The term $\varepsilon_{(i)}$ represents the residual error between the i^{th} proxy observation and the proxy model. The term C represents the cleaning methodology employed (BCP = 0, Reductive = 1) and the coefficient α_4 is the cleaning offset between data sets cleaning according to the BCP and reductively cleaned data sets. Rewriting Bayes' rule (equation (1)) for the Mg/Ca model:

$$\pi(\Phi | Mg/Ca, T, S, \Delta CO_3^{2-}, C) \propto f(Mg/Ca | T, S, \Delta CO_3^{2-}, C, \Phi) \cdot \pi(\Phi) \tag{3}$$

The vector Φ represents the regression coefficients (α_1, α_2, α_3, α_4, and α_0) and the variance on the regression τ^2.

3.1. Prior Distributions

For mathematical closure, Bayesian inference requires the specification of prior distributions, which can be subjective in nature. These priors encode our scientific understanding about the parameters before we have observed the current data. Sediment trap [e.g., *Anand et al*., 2003], culturing [*Kisakürek et al*., 2008], and core-top studies [e.g., *Dekens et al*., 2002] have all reported a temperature sensitivity of 7–10%/°C,

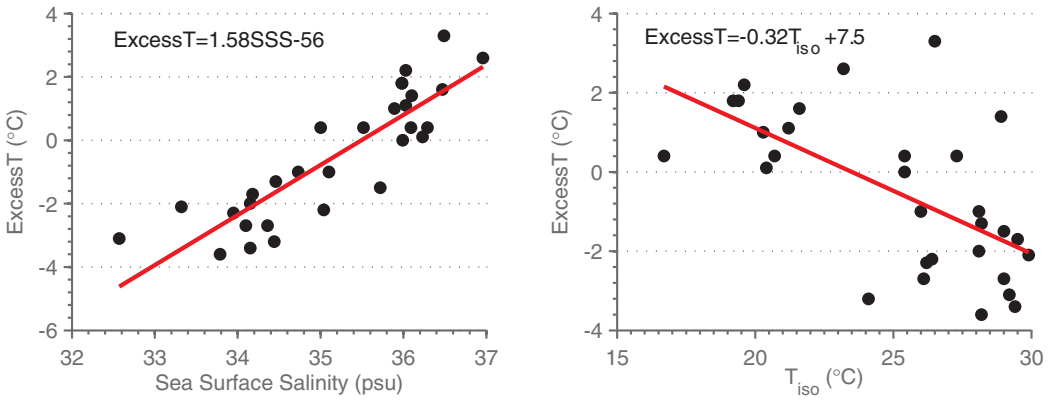

Figure 2. "Excess Temperature." (left) "ExcessT" as a function of SSS for the *Mathien-Blard and Bassinot* [2009] data set. *Mathien-Blard and Bassinot* [2009] calculated "ExcessT" as the difference between SST inferred from Mg/Ca, using the *Anand et al.* [2003] *G. ruber* specific equation (Mg/Ca = 0.449exp(0.09T)), and the isotopic temperature (T_{iso}), inferred from the *Shackleton* [1974] equation and $\delta^{18}O_{sw}$ estimates from the *LeGrande and Schmidt* [2006] gridded data set. They showed a significant positive relation between "excessT" and SSS. (right) "ExcessT" as a function of T_{iso}. We find a significant negative relation between the two quantities, implying that the inferred "ExcessT"-SSS relationship may be biased.

which we will use as a basis to build our prior distribution on the sensitivity to temperature. Although both culturing [*Hönisch et al.*, 2013; *Kisakürek et al.*, 2008; *Lea et al.*, 1999] and core-top [*Arbuszewski et al.*, 2010; *Mathien-Blard and Bassinot*, 2009; *Sadekov et al.*, 2009] studies have reported a salinity effect on *G. ruber* Mg/Ca, these studies disagree on the magnitude of the salinity influence. *Mathien-Blard and Bassinot* [2009] and *Arbuszewski et al.* [2010] both reported a large salinity sensitivity (15%/psu and 27%/psu, respectively) compared to the sensitivity deduced from culturing experiments (3–6%/psu) [*Hönisch et al.*, 2013; *Kisakürek et al.*, 2008].

Mathien-Blard and Bassinot [2009] hypothesized that this discrepancy could reflect the additional stress on *G. ruber* individuals in laboratory settings, which could alter the calcification process, or indicate a change in Mg incorporation into the test during the foraminifer's lifetime. Here, we demonstrate that this discrepancy is the result of statistical processing of the data. In their original study, *Mathien-Blard and Bassinot* [2009] defined "ExcessT" as the difference between the Mg/Ca-temperature calculated from the *Anand et al.* [2003] calibration ($T_{Mg/Ca}$) and the isotopic temperature (T_{iso}) obtained from the equation of *Shackleton* [1974] and gridded estimates of the isotopic composition of seawater $\delta^{18}O_{sw}$ [*LeGrande and Schmidt*, 2006]. They showed a significant, positive relation between "Excess T" and SSS (Figure 2) that they used to deduce a sensitivity of ~15%/psu:

$$ExcessT = T_{Mg/Ca} - T_{iso} = \frac{\ln\left(\frac{Mg/Ca}{0.449}\right)}{0.09} - T_{iso} = 1.58SSS - 56$$

Rearranging and solving for Mg/Ca:

$$Mg/Ca = \exp\left(0.09T_{iso} + 0.14SSS - 5.89\right)$$

However, a plot of "ExcessT" versus T_{iso} (Figure 2) for their data set reveals dependence between the two variables, suggesting that the expression based on "ExcessT" does not accurately account for the changes in Mg/Ca. A direct, nonlinear regression between Mg/Ca, T_{iso}, and SSS for this data set yields the following equation (standard error on the coefficients of the regression given in parenthesis):

$$Mg/Ca = \exp\left(0.09(\pm 0.01)T_{iso} + 0.04(\pm 0.03)SSS - 2.29(\pm 1.4)\right)$$

These results suggest that the statistical model to describe the dependence of Mg/Ca to environmental parameters should use a direct calibration technique rather than rely on residual analysis. Furthermore, the 4%/psu salinity sensitivity is in good agreement with culturing studies. Using core-top data sets from the Atlantic, *Arbuszewski et al.* [2010] reported a larger salinity sensitivity of 27%/psu. This observation is based on elevated Mg/Ca ratios in the subtropical Atlantic compared to the ratios in tropical samples. Based on shell weight analyses and SEM images from a subset of cores used in the *Arbuszewski et al.* [2010] study,

Hertzberg and Schmidt [2013] argued that these regional differences were a consequence of poor preservation in the equatorial Pacific rather than salinity, suggesting a much lower salinity sensitivity than the 27%/psu reported in the *Arbuszewski et al*. [2010] study. Finally, the core-top study from *Sadekov et al*. [2009] supports a sensitivity of 6%/psu in better agreement with culturing studies. Therefore, we will ignore the results of *Arbuszewski et al*. [2010] in setting the priors of our multivariate calibration.

Hönisch et al. [2013] combined new culture data on *G. ruber* (pink) with those of *Kisakürek et al*. [2008] to derive their reported 3.3 ± 1.7%/psu (95% confidence interval) salinity sensitivity. This low sensitivity value is primarily driven by the inclusion of the high-salinity datapoint of *Kisakürek et al*. [2008]. However, *Kisakürek et al*. [2008] excluded this value in their study since their experiment was not setup to properly control pH changes at such high salinities. Doing so yields a sensitivity value of 4.7 ± 1.7%/psu for the combined data set in agreement with the value reported by *Kisakürek et al*. [2008]. Since the value of the regression constant (α_0 in our model, equation (2)) is correlated to the temperature and salinity sensitivities, we use the results of the multivariate regression of *Kisakürek et al*. [2008] as priors for the α_0, α_1, and α_2 coefficients.

Using a global data set comprising 79 core-top samples, *Regenberg et al*. [2014] inferred a decrease in the Mg/Ca ratio of planktonic foraminiferal shells of 5.4 ± 3.8%/μmol.kg^{-1} below a critical ΔCO_3^{2-} threshold of ~21 μmol/kg, which we use in our calibration model (α_3, equation (2)). Since this sensitivity to dissolution is derived from core-top samples that are not included in the present study, we use the results of *Regenberg et al*. [2014] as a prior for the current calibration. For the cleaning parameter, we use a vague, uninformed prior (uniform distribution) representing the paucity of systematic studies on the subject. Taking these various results into account, we set the priors on the coefficients as (Figure 2):

$$\alpha_0 \sim N(-2.8, 0.5)$$
$$\alpha_1 \sim N(0.08, 0.01)$$
$$\alpha_2 \sim N(0.06, 0.01)$$
$$\alpha_3 \sim N(0.054, 0.019)$$
$$\alpha_4 \sim U(0, 0.4)$$
$$1/\tau^2 \sim Ga(1.0, 0.1)$$

where $N(\mu, \sigma)$ represents a normal distribution centered around mean μ and standard deviation σ, $U(a, b)$ represents a uniform distribution over the interval [a,b], and $Ga(k, \beta)$ represents a gamma distribution with shape parameter k and rate parameter β. The use of Gaussian priors for α_0, α_1, α_2, and α_3 reflects the amount of scientific information available before we observed the data, justifying the use of relatively informed priors for these sensitivity coefficients. The regression was performed using the JAGS software package for Bayesian inference (http://mcmc-jags.sourceforge.net). JAGS uses the precision rather than the variance in the regression, which is expressed as $1/\tau^2$ and is represented by the variable called "pre" in the supporting information Softwares S1 and S2. Because the MCMC algorithm may take a while to converge, we initialize the calculation by using the mean values of the normal distributions and the midpoint value of the uniform distribution. To check for convergence, we use two chains that were run for 110,000 steps. As it is commonly done, the final marginal posterior distributions (Figure 3) are derived from one chain, neglecting the first 10,000 "burn-in" trials, which are used to establish the location of the posterior, and including every 20th step to prevent serial auto-correlation among the values of the regression coefficients. This process results in 10,000 sets of coefficients (supporting information Table S2), which are used to evaluate the uncertainty.

3.2. Posterior Distributions: Mg/Ca Sensitivity to Temperature, Salinity, and Dissolution

The posterior distributions are shown in Figure 3. The inferred sensitivities ($\pm 2\sigma$) to temperature, salinity, and deep-water ΔCO_3^{2-} are 8.7 ± 0.9%/°C, 3.9 ± 1.2%/psu, and 3.3 ± 1.25%/μmol.kg^{-1} respectively. Our inferred temperature sensitivity is similar to the canonical 9%/°C obtained from different calibration methods. The salinity sensitivity reported here is lower than that reported from other core-top studies (5.7%/psu) [*Sadekov et al*., 2009] but agrees with laboratory experiments designed to isolate the salinity effect on Mg/Ca (4–5%/psu) [*Kisakürek et al*., 2008; *Lea et al*., 1999]. Our data also suggest a lower sensitivity to dissolution than that reported by *Regenberg et al*. [2014], which we use as prior in the current calculation. Taken together, our results support the current understanding that temperature is the dominant control on *G. ruber* Mg/Ca. We also find that the cleaning offset between the BCP and the reductive method is 11 ± 4.9%, in agreement with

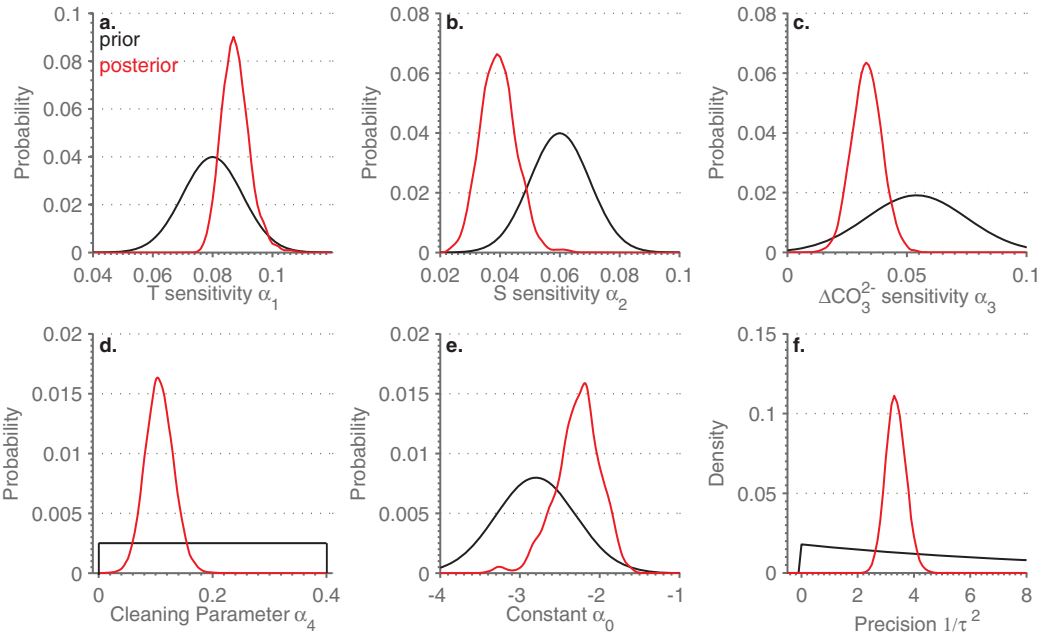

Figure 3. Probability distribution of the sensitivity parameters. Prior (black) and posterior (red) probability functions for the Mg/Ca sensitivity to (a) temperature, (b) salinity, (c) dissolution (expressed here as deep-water ΔCO_3^{2-}); (d) Regression constant in the Mg/Ca model equation (2). (e) Cleaning parameter used to adjust the reductively cleaned data sets. (f) Precision ($1/\tau^2$) on the regression.

laboratory experiments [*Rosenthal et al.*, 2004] and the often cited 10% used for data correction [*Arbuszewski et al.*, 2010]. The inferred standard deviation on Mg/Ca is $\tau = 0.55 \pm 0.06$ mmol/mol. This variance includes uncertainty from Mg/Ca analysis (both from sample heterogeneity and instrument, which we estimated to be about 0.2 mmol/mol for the samples measured in this study), as well as inter-laboratory offsets not associated with cleaning and the additional scatter from the assumption that Mg/Ca reflects modern conditions. Therefore, this spatial estimate of the variance made on globally distributed core-top samples (i.e., "spatial" τ^2), is larger than expected from downcore measurements (i.e., "temporal" τ^2) from a single location performed in the same laboratory, within the same sedimentary settings, and not including the scatter introduced by the representation of Holocene data as 20th century conditions. Therefore, we recommend using a "temporal" τ for downcore predictions of temperature, salinity, or ΔCO_3^{2-} that would more accurately reflect the analytical uncertainty associated with the record. Excluding the data sets with mixed *G. ruber* morphotypes does not affect the results presented here (supporting information Text S1).

Although our results produce similar average sensitivities as studies that considered these different influences separately, using a multivariate regression allows us to preserve the dependence among the coefficients. In a regression, the sensitivity coefficients and the constant are correlated. Indeed, we find a strong anti-correlation between the constant α_0 and the temperature and salinity sensitivity coefficients α_1, α_2 (-0.8 and -0.9, respectively). We also find a positive correlation between the temperature sensitivity α_1, and the salinity and dissolution sensitivities α_2, α_3 ($\sim$0.4) as well as a negative correlation between the dissolution parameter α_3 and the cleaning parameter α_4, which would be expected. Therefore, randomly selecting coefficients from the posterior distributions (or from distributions obtained in previous studies) would not necessarily provide valid calibration equations that could represent the data.

4. Prediction Model: Accuracy in Modern Settings and Sensitivity to Prior Information

4.1. Temperature

Inverting the calibration model allows one to make predictions of the environmental parameters (temperature, salinity, deep-water ΔCO_3^{2-}). When the functional model involves only one regressor, then the inverse model can be solved without the need for additional information. However, in the case of the Mg/Ca model

described in equation (2), predicting one environmental parameter (e.g., temperature) requires additional knowledge about changes in the other two parameters (salinity and ΔCO_3^{2-} in the current example). For temperature, the prediction model then takes the form:

$$\pi\left(T|Mg/Ca, S, \Delta CO_3^{2-}, C, \Phi\right) \propto f\left(Mg/Ca|T, S, \Delta CO_3^{2-}, C, \Phi\right) \cdot \pi(T) \quad (4)$$

where the likelihood function $f\left(Mg/Ca|T, S, \Delta CO_3^{2-}, C, \Phi\right)$ has the same form as in equation (3) and the parameters Φ are taken from the calibration model. To test the accuracy of our model in modern settings, we predict temperature for each of the core-top locations used in the calibration given their calibration salinity and deep-water ΔCO_3^{2-}. To allow for Bayesian inference on the prediction model, we also need to provide a prior for temperature. For the calibration model, we derived our priors from previous studies who quantified the influence of these environmental parameters. However, deriving a prior for temperature presents the added difficulty that although a guess in modern settings can be guided by instrumental databases such as the WOA13, this prior may not be applicable in the past when conditions are expected to be very different. Therefore, we need to investigate the sensitivity of our prediction model to the prior on temperature.

To do so, we constructed four priors representing various degree of confidence in our belief before we observe the data. The first two priors are normal distributions centered around the modern mean value at each core-top location with standard deviations of 2°C and 4°C respectively (Figures 4a and 4b). These priors represent a firm belief in the location of the average temperature but decreased confidence in the spread around this mean value. The precision and accuracy of the prediction model is then assessed as the 95% CI width from the Bayesian calculation and the Root Mean Square Error (RMSE) between the median predicted temperature and the calibration temperature respectively. When using a prior centered around the mean value, the accuracy is 0.9°C and 1.3°C for a prior with a standard deviation of 2°C and 4°C respectively. In other words, the accuracy on the estimates increases (RMSE decreases) if the prior distribution is tightly centered around the mean value. The precision on the SST estimates is 5°C ($\sigma = \pm 1.3$°C) and 6°C ($\sigma = \pm 1.5$°C) respectively, in line with previous calibrations [*Anand et al*., 2003; *Dekens et al*., 2002].

The third prior is a normal distribution centered around 22°C and a standard deviation of 4°C (Figure 3c). We use this prior to test the accuracy and the precision of the estimates with a poor initial guess of temperature. Although the precision on the temperature estimates is not affected by the choice of mean for the prior distribution, the accuracy on the mean estimates decreases slightly (RMSE increases from 1.3°C to 1.7°C). In the extreme case where no prior information on SST can be obtained, we suggest running the algorithm with a uniform prior, bound by the calcification range of *G. ruber* (Figure 4d). Doing so results in an accuracy of 1.8°C and a precision of 7°C ($\sigma = \pm 1.7$°C).The residuals between the median calculated temperature from the prediction model and the calibration temperatures (supporting information Text S1) follow a Gaussian distribution centered around zero. Furthermore, we observe no significant relationship between the residuals and latitude (supporting information Text S1). Our results suggest that although the accuracy and precision on the SST estimates are slightly influenced by the choice of the prior distribution, our new calibration equation can provide accurate estimates in modern settings even for a poor initial guess of the SST value at the core site.

This calculation assumes that the estimates of salinity and ΔCO_3^{2-} are accurate and precise. In modern settings, these parameters can be obtained from hydrographic data, which therefore satisfies this assumption. In paleoceanographic studies, these estimates would likely be uncertain, increasing the error on the temperature estimates. Furthermore, a systematic deviation from the accurate salinity and ΔCO_3^{2-} values would also create a bias in the temperature estimates.

4.2. Salinity

For salinity, the prediction model takes the form:

$$\pi\left(S|Mg/Ca, T, \Delta CO_3^{2-}, C, \Phi\right) \propto f\left(Mg/Ca|T, S, \Delta CO_3^{2-}, C, \Phi\right) \cdot \pi(S) \quad (5)$$

where the likelihood function $f\left(Mg/Ca|T, S, \Delta CO_3^{2-}, C, \Phi\right)$ has the same form as in equation (3) and the parameters Φ are taken from the calibration model. We follow the same framework as for temperatures as we test the precision and accuracy of our model using different salinity priors representing the degree of confidence in our prior belief about salinity before observing the data.

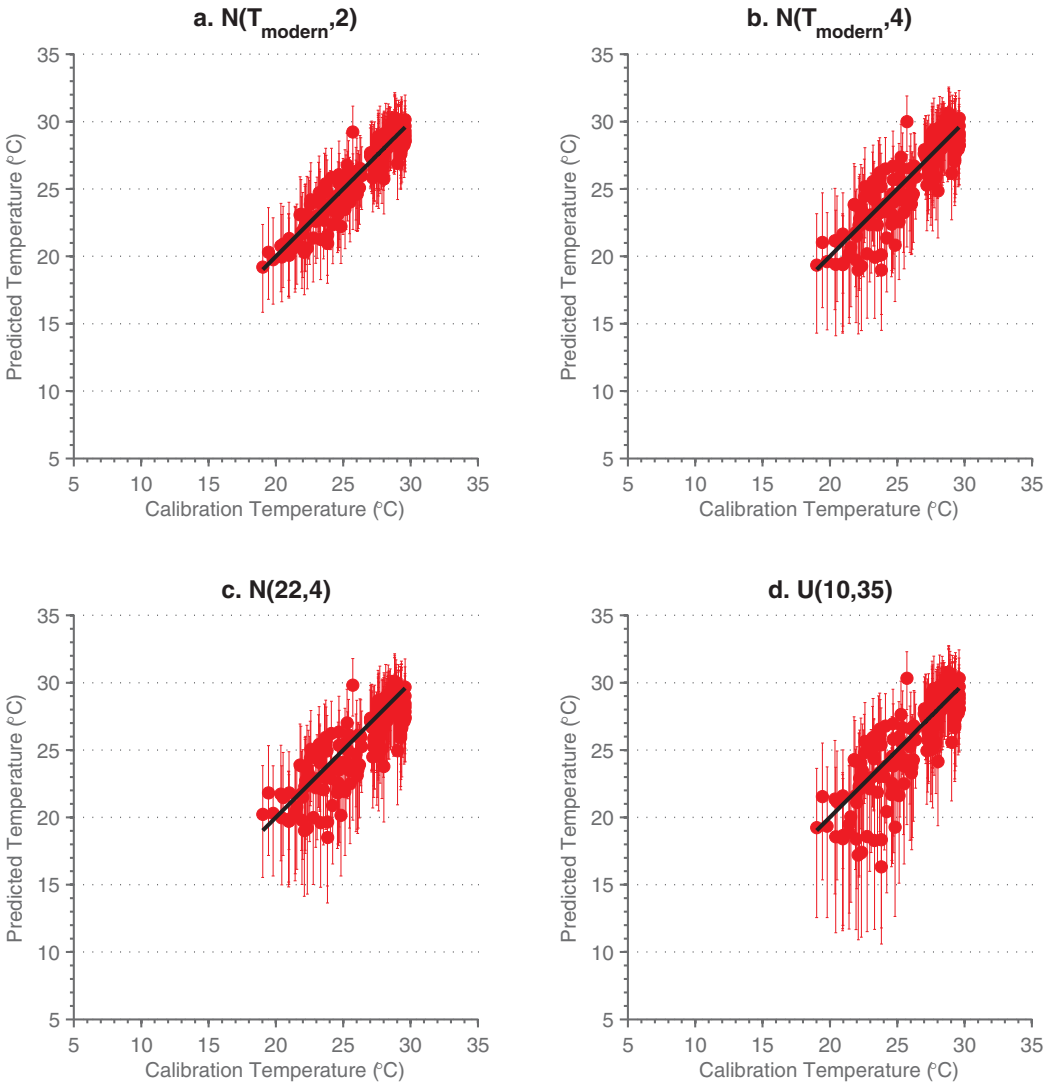

Figure 4. Accuracy in modern settings—Temperature. Predicted versus WOA13 temperature for the core-top samples considered in this study (n = 186). We used different priors representing various degrees of confidence in the prior knowledge about the temperature. (a) Normal prior centered around modern WOA13 temperature at each core-top location and a standard deviation of 2°C. (b) Normal prior centered around modern WOA13 temperature at each core-top location and a standard deviation of 4°C. (c) Normal prior centered around 22°C at each core-top location and a standard deviation of 4°C. (d) Uniform prior representing calcification range of *G. ruber*.

First, we use two normal distributions centered around the modern mean value at each core-top location with standard deviations of 0.5 psu and 1 psu respectively (Figures 5a and 5b). The accuracy of our predictive salinity model given a good initial guess of the mean salinity at the core location varies between 0.07 psu and 0.3 psu (for a prior with a standard deviation of 0.5 psu and 1 psu respectively). The precision on the salinity estimates for these priors is on the order of 2–4 psu ($\sigma = \pm 0.5$–1 psu), a value near the expected signal. Then, we use a prior centered around 35 psu at each of the core-top locations with a standard deviation of 1 psu. The use of this prior allows us to test the accuracy and precision of the prediction model given a poor initial guess of the location of the posterior salinity distributions. The results (Figure 5c) suggest that if the location of the posterior distribution is not accurately known, then the model fails to predict salinity at the core-top locations. Finally, since it may not always be possible to obtain accurate (location of the Gaussian distribution) and precise (spread) prior distribution for SSS, we also use a uniform prior across the calcification range of *G. ruber* (Figure 5d) to test the accuracy and precision of our model in modern settings. For this uniform prior, the accuracy and precision on the SSS estimates are 2.4 psu and 10 psu ($\sigma = \pm 2.5$ psu) respectively. Our results therefore suggest that (1) the accuracy of the SSS predictions is very sensitive to prior information, and (2) these predictions are not precise enough for use in routine paleoceanographic

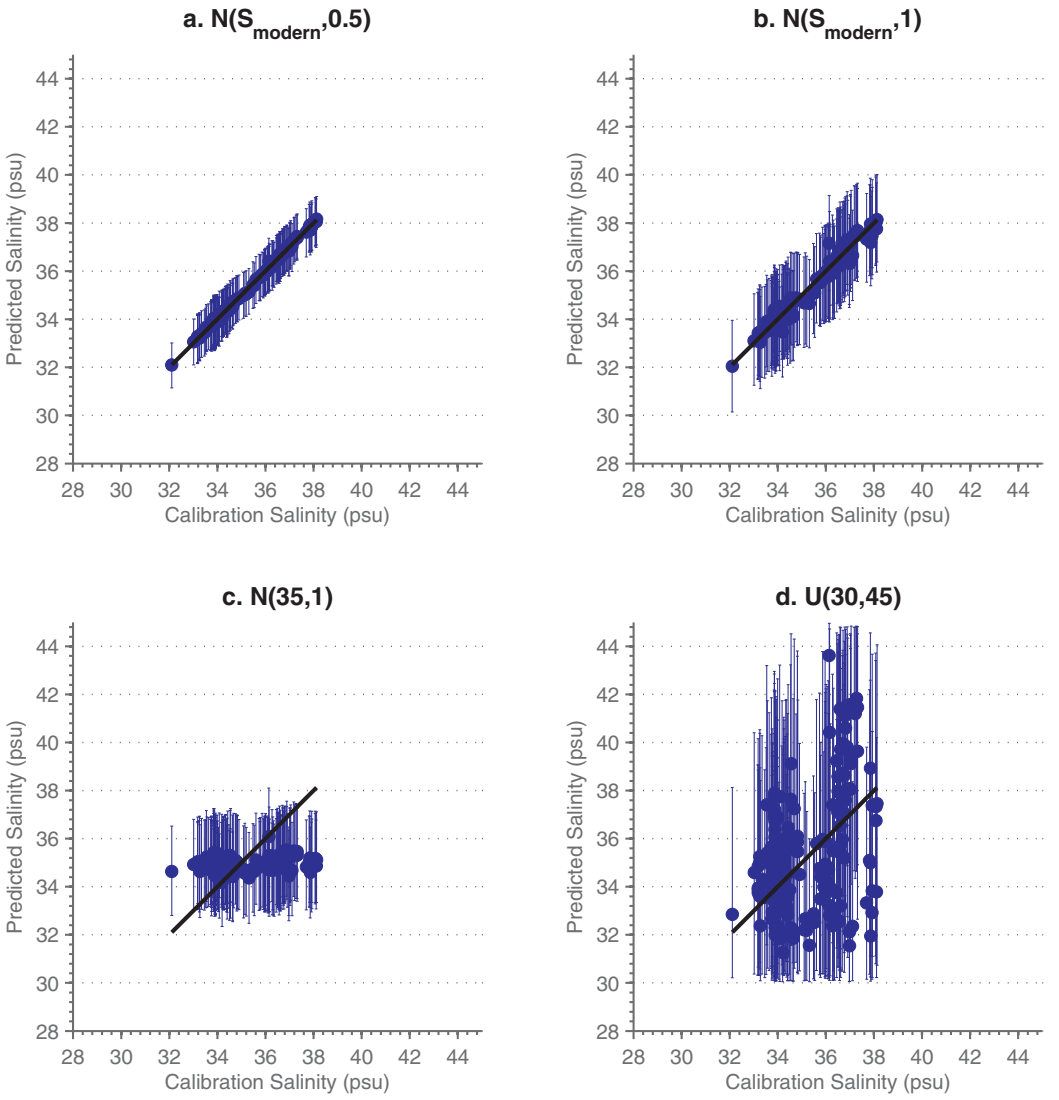

Figure 5. Accuracy in modern settings—Salinity. Predicted versus WOA13 salinity for the core-top samples considered in this study (n = 186). We used different priors representing various degrees of confidence in the prior knowledge about the salinity. (a) Normal prior centered around modern WOA13 salinity at each core-top location and a standard deviation of 0.5 psu. (b) Normal prior centered around modern WOA13 salinity at each core-top location and a standard deviation of 1 psu. (c) Normal prior centered around 35 psu at each core-top location and a standard deviation of 1 psu. (d) Uniform prior representing calcification range of *G. ruber*.

reconstructions. Our best prior estimate suggests a precision of $\pm$0.5 psu, in line with expected changes in SSS on glacial-interglacial timescales. Therefore, even if information about past temperature and deep-water ΔCO_3^{2-} could be obtained from other proxies, our model is not precise (nor accurate) enough to allow for past estimates of SSS variability.

4.3. Deep-Water ΔCO_3^{2-}

For ΔCO_3^{2-}, the prediction model takes the form:

$$\pi\left(\Delta CO_3^{2-}|Mg/Ca,T,S,C,\Phi\right) \propto f\left(Mg/Ca|T,S,\Delta CO_3^{2-},C,\Phi\right)\cdot\pi\left(\Delta CO_3^{2-}\right) \quad (6)$$

where the likelihood function $f\left(Mg/Ca|T,S,\Delta CO_3^{2-},C,\Phi\right)$ has the same form as in equation (3) and the parameters Φ are taken from the calibration model. Because dissolution does not affect *G. ruber* Mg/Ca above a critical threshold (equation (2)), we set the maximum possible values of Mg/Ca-based ΔCO_3^{2-} to 21 μmol/kg (Figure 5). This leads to negatively skewed CIs. As with temperature and salinity, we use four different priors to test the accuracy and precision of reconstructed deep-ocean ΔCO_3^{2-} at the core-top locations.

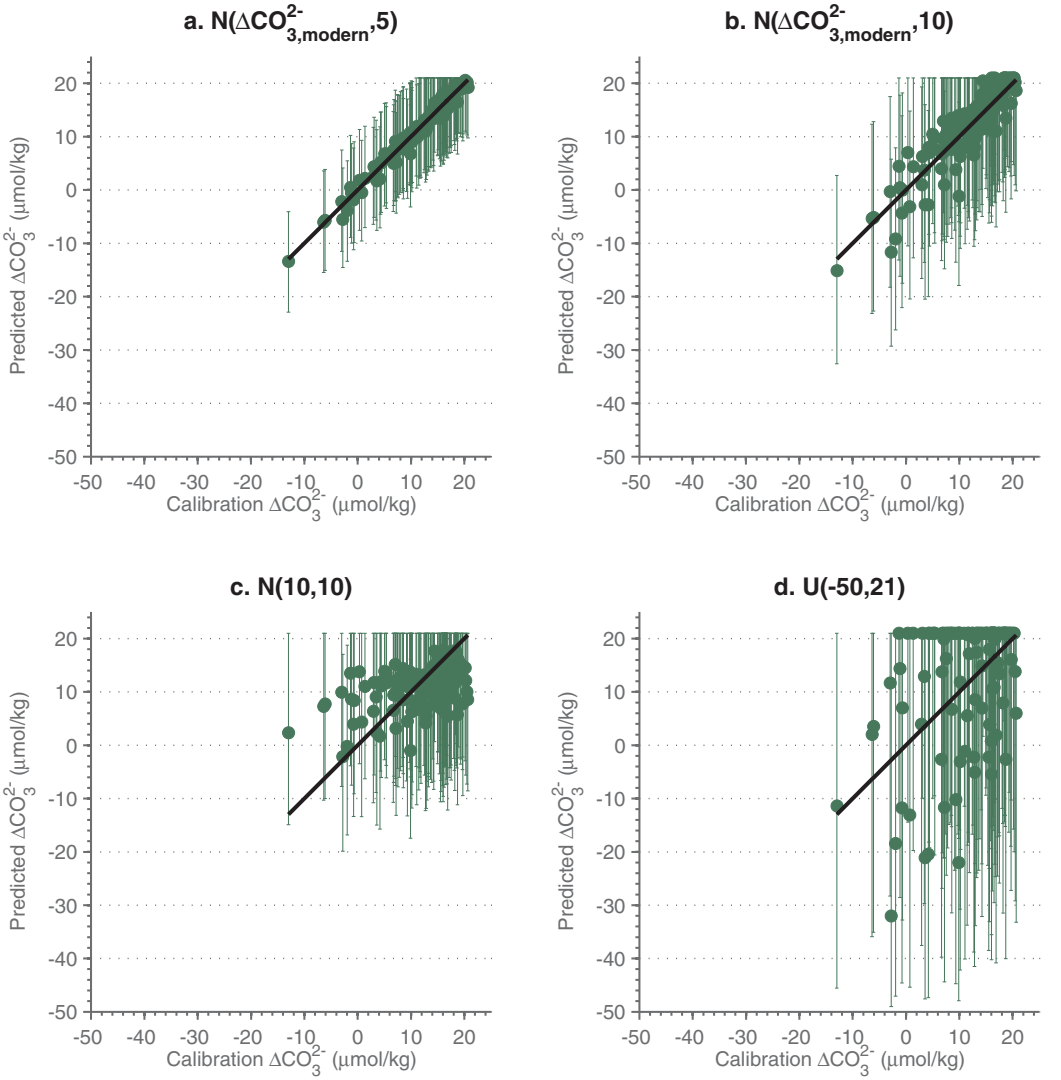

Figure 6. Accuracy in modern settings—ΔCO_3^{2-}. Predicted versus calibration ΔCO_3^{2-} for the core-top samples considered in this study (n = 186). We used different priors representing various degrees of confidence in the prior knowledge about deep-water ΔCO_3^{2-}. (a) Normal prior centered around modern deep-water ΔCO_3^{2-} at each core-top location and a standard deviation of 5 μmol/kg. (b) Normal prior centered around modern deep-water ΔCO_3^{2-} at each core-top location and a standard deviation of 10 μmol/kg. (c) Normal prior centered around 10 μmol/kg at each core-top location and a standard deviation of 10 μmol/kg. (d) Uniform prior representing a large range of environmental conditions under which *G. ruber* tests are susceptible to dissolution. Note that *G. ruber* is not susceptible to dissolution above a deep-water ΔCO_3^{2-} of 21 μmol/kg and therefore the saturation state of deep-water cannot be reconstructed from Mg/Ca above this critical concentration.

Using Gaussian priors centered around the modern mean value and standard deviations of 5 μmol/kg and 10 μmol/kg (Figures 6a and 6b) leads to an accuracy of 1 μmol/kg and 3 μmol/kg respectively and a precision of 19 μmol/kg ($\sigma = 4.8$ μmol/kg) and 37 μmol/kg ($\sigma = 9.3$ μmol/kg) respectively. Therefore, if the prior knowledge about the average deep-ocean ΔCO_3^{2-} is accurately and somewhat precisely known, it is possible to reconstruct deep-ocean ΔCO_3^{2-} variability assuming large changes in this quantity, perhaps in response to a water mass substitution at the core location. Furthermore, this exercise does not require separate knowledge of temperature and salinity variability if the reconstruction is based on Mg/Ca records from a series of cores taken along a depth transect [*Fehrenbacher and Martin*, 2011].

However, a lack of prior knowledge about past ΔCO_3^{2-} variability prevents the reconstruction of this quantity. Using a Gaussian prior centered on 10 μmol/kg with a standard deviation of 10 μmol/kg leads to inaccurate reconstructed ΔCO_3^{2-} values away from this prior estimate (Figure 6c). Similarly, using a uniform prior with a large range of deep-ocean ΔCO_3^{2-} leads to an accuracy of 23 μmol/kg and a precision of 105 μmol/kg ($\sigma = \pm 27$ μmol/kg), which may be larger than the underlying signal (Figure 6d).

5. Paleoceanographic Implications: An Example for the Western Pacific Warm Pool

5.1. Sensitivity Analysis

The recognition that salinity and deep-water ΔCO_3^{2-} have an influence on foraminiferal Mg/Ca has implications for paleoceanographic studies that attempt to reconstruct SST changes over glacial-interglacial timescales, when large SSS changes are expected due to the formation and retreat of continental ice sheets. We performed a sensitivity experiment to explore the potential bias arising from systematic changes in deep-water ΔCO_3^{2-} and SSS at a site in the Western Tropical Pacific (core MD81, 6.3°N, 125.82°E, 2114 m water depth [*Stott et al*., 2007]), which was not used in the calibration exercise. The purpose here is not to rewrite the deglacial SST evolution of the Western Pacific Warm Pool from a single location but rather to discuss the possible biases arising from omitting secondary influences in paleoceanographic reconstructions.

Modern Mg/Ca (defined in the present study as the average Mg/Ca over the last 4,000 years, using the standard error on the mean as a measure of uncertainty on the Mg/Ca measurements (i.e., the "temporal" τ), Mg/Ca = 5.22 ± 0.30 mmol/mol) was converted to SST using our prediction model on temperature with SSS and ΔCO_3^{2-} values of 34 psu and 2.6 μmol/kg respectively obtained from the WOA13 [*Locarnini et al*., 2013; *Zweng et al*., 2013] and GLODAP [*Key et al*., 2004] data sets using the procedure described in the methods section. We also explored the sensitivity to prior information by using two priors for temperature: a uniform prior over the 10–35°C temperature range, and a Gaussian prior centered around 28.5°C with a standard deviation of 2°C. The predicted modern temperature at the core location is ($\pm 2\sigma$) 29.3 ± 1.3°C and 29.1 ± 1.2°C using the uniform and Gaussian priors respectively. These values are in good agreement with the modern estimate of 29°C from WOA13 [*Locarnini et al*., 2013]. LGM Mg/Ca (represented by the average Mg/Ca value over the 19,000–23,000 year B.P. interval, Mg/Ca = 3.99 ± 0.20 mmol/mol) was converted to SST using our predictive model on SST with SSS and ΔCO_3^{2-} values varied from 33 to 36 psu (in 0.2 psu increments) and from −10 to 21 μmol/kg (in 0.5 μmol/kg increments) respectively. We purposefully included extreme scenarios in the original sensitivity analysis to explore the potential temperature bias from ignoring the secondary influences of salinity and dissolution on Mg/Ca. We further refined these scenarios using other lines of evidence at the end of this section. We also used two priors for this calculation: the first prior is uniform over the 10–35°C interval while the second prior is a Gaussian distribution centered around 26°C with a standard deviation of 2°C. The magnitude of LGM cooling depicted in Figure 7 is represented by the median of the Bayesian posteriors for each set of SSS and ΔCO_3^{2-} values while the uncertainty is expressed as the 95% CI width. The magnitude of LGM cooling ($\pm 2\sigma$) assuming no changes in SSS or deep-water ΔCO_3^{2-}, which is equivalent to ignoring secondary influences on *G. ruber* Mg/Ca, is 3.2 ± 1.6°C and 2.9 ± 1.6°C using the uniform and Gaussian priors respectively. On the other hand, the magnitude of LGM cooling ($\pm 2\sigma$) assuming an increase in SSS of 1 psu due to increased glacial ice volume alone and no changes in deep-water ΔCO_3^{2-} is 3.5 ± 1.6°C and 3.4 ± 1.6°C using the uniform and Gaussian priors respectively. Furthermore, an increase in deep-water ΔCO_3^{2-} at the LGM of 11.4 μmol/kg (consistent with a modern value at 1000 m water depth estimated from the WOA13 [*Locarnini et al*., 2013; *Zweng et al*., 2013] and GLODAP [*Key et al*., 2004] data sets using the procedure described in the methods section) results in a LGM cooling of 4.7 ± 1.7°C and 4.5 ± 1.6°C using the uniform and Gaussian priors respectively. Conversely, a decrease in deep-water ΔCO_3^{2-} at the LGM of 5 μmol/kg (consistent with a modern value at 3000 m water depth) results in a LGM cooling of 3.0 ± 1.6°C and 2.9 ± 1.5°C using the uniform and Gaussian priors respectively. This sensitivity experiment highlights the potential bias from ignoring the secondary influence of salinity and deep-water ΔCO_3^{2-} on Mg/Ca thermometry. Furthermore, these errors are likely correlated since these secondary factors are expected to covary in the climate system. For instance, temperature and salinity changes are anticorrelated on glacial-interglacial timescales.

Multiproxy approaches, which would allow one to deconvolve each of these secondary influences on *G. ruber* Mg/Ca, may prove useful in deriving SST estimates. *Mathien-Blard and Bassinot* [2009] and *Arbuszewski et al*. [2010] proposed a correction procedure for the effect of salinity on Mg/Ca in which they take advantage of the dual influence of temperature and salinity on both $\delta^{18}O_c$ and Mg/Ca. However, this procedure requires a set of assumptions that needs to be independently verified for each location. In particular, this procedure assumes that the spatial $\delta^{18}O_{sw}$-SSS relationship has remained constant in the past, an hypothesis that may not be accurate, especially at higher latitudes [*LeGrande and Schmidt*, 2011]. Furthermore, *LeGrande and Schmidt* [2011] argue, based on transient GCM simulations, that the slope of the spatial $\delta^{18}O_{sw}$-SSS relationship is not appropriate to describe temporal changes in SSS inferred from $\delta^{18}O_{sw}$.

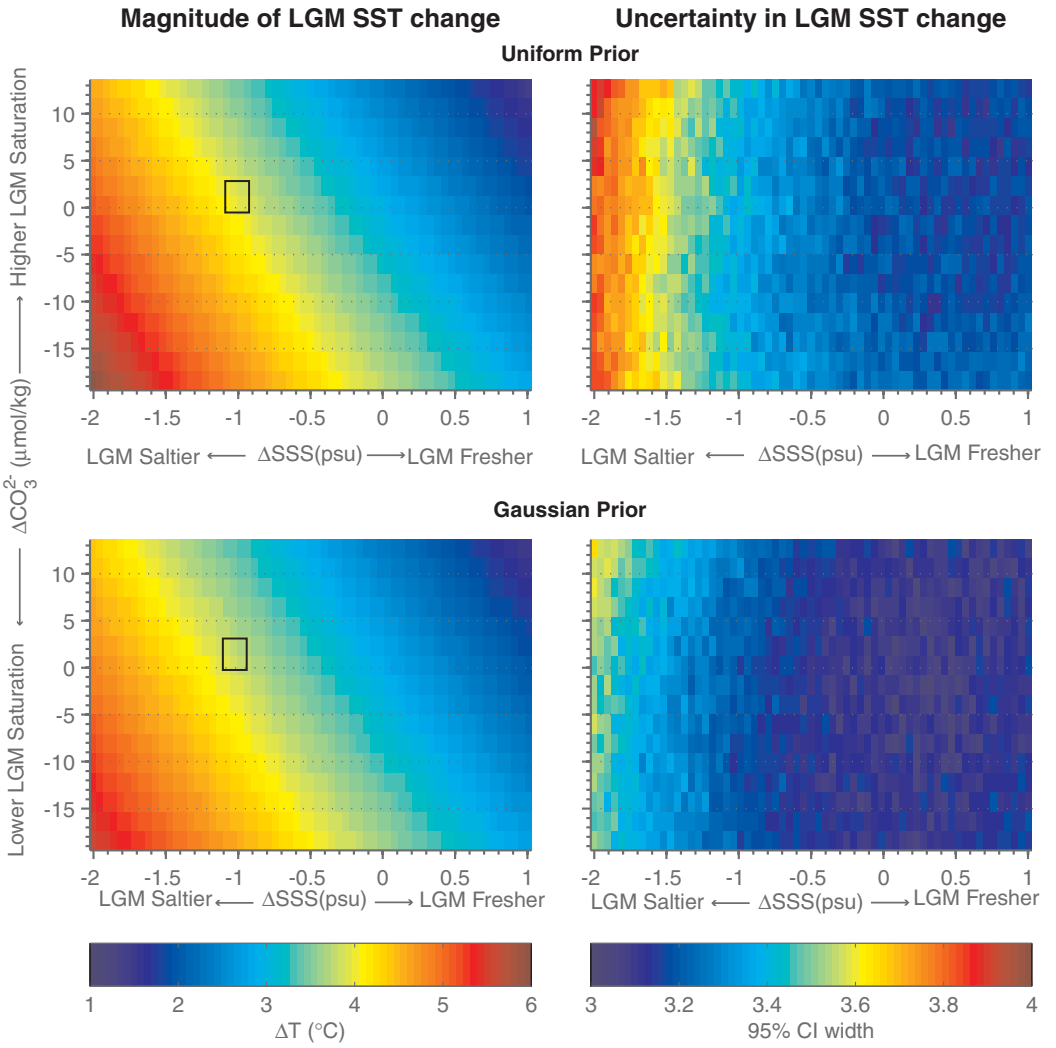

Figure 7. Sensitivity Experiment — Magnitude of LGM cooling in the Western Equatorial Pacific. (left) Magnitude of LGM cooling in response to prescribed SSS and deep-water ΔCO_3^{2-} changes at the LGM for (top) a uniform prior representing the calcification range of *G. ruber* and (bottom) a normal prior centered around 28.5°C in the modern and 26°C at the LGM with a standard deviation of 2°C. The record is from the Western Equatorial Pacific (core MD98–2181, 6.3°N, 125.82°E, 2114 m water depth [*Stott et al*., 2007]). (right) 95% CI width on the magnitude of LGM cooling. The black rectangle represents the most probable scenarios given additional lines of evidence from measured planktonic $\delta^{18}O_c$ in the same core and a nearby dissolution study [*Fehrenbacher and Martin*, 2014].

However, this assumption is vital to develop a first-order calibration equation for paired measurements of Mg/Ca and $\delta^{18}O_c$. Finally, the $\Delta\delta^{18}O_g$-ΔSSS relationship due to ice volume carries some uncertainty associated with (1) the change in global sea level estimate, (2) local deviation from eustatic sea level change, (3) uncertainty in the $\delta^{18}O_{sw}$ enrichment attributed to ice volume [*Adkins and Schrag*, 2003; *Duplessy et al*., 2002; *Fairbanks*, 1989; *Labeyrie et al*., 1987; *Schrag et al*., 1996], and (4) the time-dependence of the $\Delta\delta^{18}O_g$-ΔSSS relationship associated with variations in the isotopic composition of the ice stored in the ice sheets [*Mix and Ruddiman*, 1984]. Therefore, a full deconvolution of the salinity and temperature effects on both Mg/Ca and $\delta^{18}O_c$ will require a better characterization of the spatiotemporal relationship between $\delta^{18}O_{sw}$ and SSS over millennial to orbital timescales. Proxies that have been previously used to evaluate changes in ocean carbonate concentration, and therefore, deep-water ΔCO_3^{2-}, include planktonic foraminiferal test weight [*Broecker and Clark*, 2001a,b], planktonic foraminiferal shell assembly [*Anderson and Archer*, 2002], and benthic foraminiferal Zn/Ca [*Marchitto et al*., 2005]. A full review of the strengths and weaknesses of these proxies is beyond the scope of the present study but they should be assessed and used in conjunction with Mg/Ca to derive quantitative SST estimates.

Table 1. Change in SST, SSS, and Predicted Mg/Ca at LGM for GFDL CM2.1 and 6 CMIP5 Models Near the Location of the MD81 Proxy

Model	SST_{pre}	SST_{LGM}	ΔT	SSS_{pre}	SSS_{LGM}	ΔS	Mg/Ca_{pre}[a]	Mg/Ca_{LGM}[a]	$\Delta Mg/Ca$
GFDL CM2.1	28.69	25.21	3.48	33.52	34.36	−0.84	4.85	3.72	1.13
NASA GISS-E2-R	28.88	26.56	2.32	32.95	33.98	−1.03	4.83	4.12	0.71
MIROC-ESM[b]	28.35	26.07	2.28	33.93	32.63	1.3	4.79	3.76	1.04
CNRM-CM5	27.56	26.22	1.34	33.32	33.94	−0.62	4.37	3.99	0.38
CCSM4	28.53	26.52	2.01	33.44	34.02	−0.58	4.77	4.11	0.66
MPI-ESM-P	28.42	26.14	2.28	34.07	34.59	0.52	4.85	4.06	0.79
IPSL-CMSA-LR	27.13	23.73	3.4	33.93	34.5	−0.57	4.33	3.30	1.03
Mean	28.20	25.73	2.47	33.54	34.23	−0.69	4.67	3.88	0.78
Standard Deviation	0.69	1.09	0.83	0.41	0.29	0.20	0.25	0.32	0.27

[a]The error on the predicted Mg/Ca from the calibration model is $\sigma = 0.6$ mmol/mol.
[b]The model set-up did not follow the PMIP3 protocol, recommending increasing the global mean ocean salinity by 1 psu [*Sueyoshi et al.*, 2013]. Therefore, we ignore the results of this model in the calculated mean and standard deviation.

Although a quantitative multiproxy approach may not be possible at this time, a qualitative use of these additional lines of evidence can help identify the most plausible scenarios from our sensitivity analysis and help refine our estimate of SST changes at the LGM. Here, we use the MD81 record as a template for this qualitative treatment. Following the same procedure as for Mg/Ca, the modern-LGM change in planktonic $\delta^{18}O_c$ is $-1.83 \pm 0.23‰$. Assuming that 1.1‰ can be attributed to global sea level changes [*Waelbroeck et al.*, 2002], then the remaining $-0.73 \pm 0.23‰$ should account for both temperature and local changes in $\delta^{18}O_{sw}$ at the core location. Assuming no contribution from local $\delta^{18}O_{sw}$, then the change in $\delta^{18}O_c$ corresponds to a temperature change of 3.5 ± 1.1°C, in good agreement with the inferred change from Mg/Ca with an hypothesized change of 1 psu and no change in deep-water ΔCO_3^{2-} at the LGM. The latter is consistent with the results of *Fehrenbacher and Martin* [2011] and *Yu et al.* [2010]. Therefore, we argue that the most probable cooling at the LGM at the MD81 location is on the order of 3.5°C. It should be noted, however, that small changes in local salinity and deep-water ΔCO_3^{2-} cannot be discounted at this time. However, based on our qualitative comparison between the Mg/Ca and $\delta^{18}O_c$ data, it is unlikely that large variations in these parameters occurred at the LGM.

5.2. Implication for Model-Data Comparison

The influence of salinity and ΔCO_3^{2-} on *G. ruber* Mg/Ca prevents the direct use of the temperature estimates from this proxy for model-data comparison. Here, we explore the possibility of using the calibration model to derive predictions of Mg/Ca based on the model outputs that can be compared to the data. To do so, we calculated modern and LGM Mg/Ca based on the temperature and salinity outputs from the GDFL CM2.1 and 6 CMIP5 models near the location of the MD81 proxy (Table 1) and modern deep-water ΔCO_3^{2-} at the core location (2.6 μmol/kg). Since the models under-predict both the mean annual SST and SSS at the core location, it is not surprising that the multimodel ensemble Mg/Ca mean is lower than the measured modern Mg/Ca (4.67 ± 0.25 mmol/mol versus 5.22 ± 0.3 mmol/mol, uncertainties expressed as the standard error on the mean), although within the 2σ uncertainty envelope on the predicted and measured Mg/Ca values. Using salinity and temperature values from WOA13 [*Locarnini et al.*, 2013], the predicted modern Mg/Ca values at the MD81 location is 5.1 ± 0.6 mmol/mol, in line with the measured value.

Predicted LGM Mg/Ca from the model outputs and modern deep-water ΔCO_3^{2-} is 3.88 ± 0.32 mmol/mol, in good agreement with the measured value of 3.99 ± 0.2 mmol/mol. Therefore, the models predict a smaller Mg/Ca change between the LGM and the present than is observed in the MD81 proxy record (Table 1, 0.78 ± 0.27 mmol/mol versus 1.23 ± 0.79 mmol/mol). This discrepancy may stem from: (1) the models do not accurately represent the temperature and salinity changes between modern and LGM conditions regardless of systematic errors in the absolute temperature and salinities, and/or (2) the discrepancy in the magnitude of the Mg/Ca change can be attributed to changes in deep-water ΔCO_3^{2-} at the LGM. The change in deep-water ΔCO_3^{2-} necessary to account for the 0.45 ± 0.83 mmol/mol discrepancy is 14 ± 27 μmol/kg. Considering the modern water masses configuration at the MD81 location, such a large increase in ΔCO_3^{2-} at the LGM is unlikely. Therefore, the model-data mismatch is more likely due to a combination of the two factors mentioned previously rather than proxy uncertainty alone.

Resolving model-data discrepancies will require a set of records from different locations, especially from shallow marine settings where *G. ruber* Mg/Ca is not influenced by dissolution. The purpose of this exercise

was not to assess the validity of the models at the LGM based on a single location but rather provide a framework for future model-data comparison, which takes into account biases on the Mg/Ca proxy arising from the secondary effects of salinity and deep-water ΔCO_3^{2-}. Specifically, it may be more useful to transform the model outputs in the measured proxy than trying to deconvolve the various environmental influences on *G. ruber* Mg/Ca. A proxy system model [*Evans et al*., 2013] for foraminiferal Mg/Ca is not currently available, but would be key to improving our calibration and such data-model comparisons.

6. Conclusions

In this study, we presented a new Bayesian calibration model for *G. ruber* Mg/Ca that explicitly takes into account the effect of temperature, salinity, dissolution (expressed here as deep-water ΔCO_3^{2-}), and laboratory techniques. We found that the sensitivity ($\pm 2\sigma$) to temperature, salinity, and deep-water ΔCO_3^{2-} is $8.7 \pm 0.9\%/°C$, $3.9 \pm 1.2\%/psu$, and $3.3 \pm 1.3\%/\mu mol.kg^{-1}$, respectively, in line with previous studies [*Anand et al*., 2003; *Dekens et al*., 2002; *Hönisch et al*., 2013; *Kisakürek et al*., 2008; *Lea*, 1999; *Regenberg et al*., 2014]. Furthermore, the average offset associated with the various cleaning methodologies is $11 \pm 4.9\%$, in good agreement with the often-used value of 10%. Our results suggest that although temperature is the dominant control of *G. ruber* Mg/Ca, SST estimates can be severely biased if the salinity and deep-water ΔCO_3^{2-} changes are expected to be large.

The Bayesian framework also provides the advantage that the calibration error can be directly propagated into past estimates of these environmental parameters. A test of accuracy and precision in modern settings suggests that our new calibration model can be useful for predicting temperatures given an estimate of salinity and deep-water ΔCO_3^{2-}. However, our model is not precise or accurate enough to resolve small changes in salinity and deep-water ΔCO_3^{2-} given changes in the other two environmental parameters.

To illustrate the potential bias from ignoring secondary effects on Mg/Ca, we applied our prediction model to a published sedimentary record from the western tropical Pacific [*Stott et al*., 2007] using various estimates of SSS and deep-water ΔCO_3^{2-}. The results of this sensitivity experiment suggest that both salinity and deep-water ΔCO_3^{2-} emerge as a main source of bias in Mg/Ca paleothermometry. A complete multiproxy approach is not possible as this time. However, when constraints on SSS and deep-water ΔCO_3^{2-} can be obtained from additional sources, our calibration model can help refine past SST variability by proving probable scenarios.

Acknowledgments

The authors would like to thank Miguel Rincon (USC) for help with the analyses and Ellen Roosen (WHOI) and Robert Thunell (University of South Carolina) for providing some of the core-top samples analyzed in this study. We would also like to thank Michael Erb (UT Austin) for help with model outputs. The new geochemical data presented in this work can be found in supporting information Table S1. The JAGS routines can be found in supporting information Softwares S1 and S2. A user-friendly version of the prediction and calibration model is archived at https://github.com/khider/JAGS_MgCa. This work was funded by National Science Foundation grants ATM-0902507 (Stott) and DMS1025464 (Emile-Geay), and the U.S. Department of Energy Office of Science grants DE-SC0006985 (Jackson) and DE-SC0010843 (Huerta). Khider was supported by a postdoctoral fellowship from the University of Texas Institute for Geophysics.

References

Adkins, J. F., and D. P. Schrag (2003), Reconstructing the Last Glacial Maximum bottom water salinities from deep-sea sediment pore fluid profiles, *Earth Planet. Sci. Lett.*, *216*, 109–123.

Anand, P., H. Elderfield and M. H. Conte (2003), Calibration of Mg/Ca thermometry in planktonic foraminifera from a sediment trap time series, *Paleoceanography*, *18*(2), 1050, doi:10.1029/2002PA000846.

Anderson, D. M., and D. Archer (2002), Glacial-interglacial stability of ocean pH inferred from foraminifer dissolution rates, *Nature*, *416*, 70–73.

Antonov, J. I., D. Seidov, T. P. Boyer, R. A. Locarnini, A. V. Mishonov, and H. E. Garcia (2010), Volume 2: Salinity, in *World Ocean Atlas 2009*, Ed. NOAA Atlas NESDIS 69, 184 pp., U.S. Gov. Print. Off., Washington, D. C.

Arbuszewski, J., P. DeMenocal, A. Kaplan and E. C. Farmer (2010), On the fidelity of shell-derived $\delta^{18}O_{seawater}$ estimates, *Earth Planet. Sci. Lett.*, *300*, 186–196.

Barker, S., M. Greaves, and H. Elderfield (2003), A study of cleaning procedures used for foraminiferal Mg/Ca paleothermometry, *Geochem. Geophys. Geosyst.*, *4*(9), 8407, doi:10.1029/2003GC000559.

Barker, S., I. Cacho, H. Benway, and K. Tachikawa (2005), Planktonic foraminiferal Mg/Ca as a proxy for past oceanic temperatures: A methodological overview and data compilation for the Last Glacial Maximum, *Quat. Sci. Rev.*, *24*, 821–834.

Berger, W. H., M. C. Bonneau, and F. L. Parker (1982), Foraminifera on the deep-sea floor: Lysocline and dissolution rate, *Oceanol. Acta*, *5*, 249–258.

Berliner, L., R. Levine, and D. Shea (2000a), Bayesian climate change assessment, *J. Clim.*, *13*, 3805–3820.

Berliner, L., C. K. Wikle, and N. Cressie (2000b), Long-lead prediction of Pacific SSTs via Bayesian Dynamic Modeling, *J. Clim.*, *13*, 3953–3968.

Blaauw, M., and J. A. Christen (2011), Flexible paleoclimate age-depth models using an autoregressive gamma process, *Bayesian Anal.*, *6*(3), 457–474.

Broecker, W. S., and E. Clark (2001a), Reevaluation of the $CaCO_3$ size index paleocarbonate ion proxy, *Paleoceanography*, *16*, 669–671.

Broecker, W. S., and E. Clark (2001b), Glacial-to-Holocene redistribution of carbonate ion in the deep sea, *Science*, *294*, 2152–2155.

Brown, S., and H. Elderfield (1996), Variations in Mg/Ca and Sr/Ca ratios of planktonic foraminifera caused by postdepositional dissolution: evidence of shallow Mg-dependent dissolution, *Paleoceanography*, *11*, 543–551.

Debret, M., V. Bout-Roumazeilles, F. Grousset, M. Desmet, J. F. McManus, N. Massel, D. Sebag, J. R. Petit, Y. Copard, and A. Trentesaux (2007), The origin of the 1500-year climate cycles in Holocene North Atlantic records, *Clim. Past Discuss.*, *3*, 679–692.

Dekens, P. S., D. W. Lea, D. K. Pak, and H. J. Spero (2002), Core top calibration of Mg/Ca in tropical foraminifera: Refining paleotemperature estimation, *Geochem. Geophys. Geosyst.*, *3*(4), 1022, doi:10.1029/2001GC000200.

de Villiers, S. (2003), Dissolution effects on foraminiferal Mg/Ca records of sea surface temperature in the western equatorial Pacific, *Paleoceanography*, *18*(3), 1070, doi:10.1029/2002PA000802.
Dueñas-Bohorquez, A., R. E. da Rocha, A. Kuroyanagi, J. Bijma, and G.-J. Reichart (2009), Effect of salinity and seawater calcite saturation state on Mg and Sr incorporation in cultured planktonic foraminifera, *Mar. Micropaleontol.*, *73*, 178–189.
Duplessy, J. C., L. Labeyrie, and C. Waelbroeck (2002), Constraints on the ocean oxygen isotopic enrichment between the Last Glacial Maximum and the Holocene: Paleoceanographic implications, *Quat. Sci. Rev.*, *21*, 315–330.
Elderfield, H., and G. Ganssen (2000), Past temperature and δ^{18}O of surface ocean waters inferred from foraminiferal Mg/Ca ratios, *Nature*, *405*, 442–445.
Elderfield, H., C. J. Bertram, and J. Erez (1996), A biomineralization model for the incorporation of trace elements into foraminiferal calcium carbonate, *Earth Planet. Sci. Lett.*, *142*, 409–423.
Elderfield, H., M. Vautravers, and M. Cooper (2002), The relationship between shell size and Mg/Ca, Sr/Ca, δ^{18}O, and δ^{13}C of species of planktonic foraminifera, *Geochem. Geophys. Geosyst.*, *3*(8), 1052, doi:10.1029/2001GC000194.
Evans, M. N., S. E. Tolwinski-Ward, D. M. Thompson, and K. J. Anchukaitis (2013), Applications of proxy system modeling in high resolution paleoclimatology, *Quat. Sci. Rev.*, *76*, 16–28.
Fairbanks, R. G. (1989), A 17,000-year glacio-eustatic sea level record: Influence of glacial melting rates on the Younger Dryas event and deep-ocean circulation, *Nature*, *342*(6250), 637–642.
Farmer, E. C. (2005), *Tropical Atlantic Climate Change from Mg/Ca and Oxygen Isotopes of Planktonic Foraminifera*, Columbia Univ., N. Y.
Fehrenbacher, J., and P. Martin (2011), Western equatorial Pacific deep water carbonate chemistry during the Last Glacial Maximum and deglaciation: Using planktic foraminiferal Mg/Ca to reconstruct sea surface temperature and seafloor dissolution, *Paleoceanography*, *26*, PA2225, doi:10.1029/2010PA002035.
Fehrenbacher, J., and P. Martin (2014), Exploring the dissolution effect on the intrashell Mg/Ca variability of the planktic foraminifer *Globigerinoides ruber*, *Paleoceanography*, *29*, 854–868, doi:10.1002/2013PA002571.
Friedrich, O., R. Schiebel, P. A. Wilson, S. Weldeab, C. J. Beer, M. J. Cooper, and J. Fiebig (2012), Influence of test size, water depth, and ecology on Mg/Ca, Sr/Ca, δ^{18}O and δ^{13}C in nine modern species of planktic foraminifers, *Earth Planet. Sci. Lett.*, *319-320*, 133–145.
Garcia, H. E., R. A. Locarnini, T. P. Boyer, J. I. Antonov, M. M. Zweng, O. K. Baranova, and D. R. Johnson (2010), Volume 4: Nutrients (phosphate, nitrate, silicate), in *World Ocean Atlas 2009, NOAA Atlas NESDIS 71*, edited by S. Levitus, 398 pp., U.S. Gov. Print. Off., Washington, D. C.
Gelman, A., J. B. Carlin, H. S. Stern, and D. B. Rubin (2013), *Bayesian Data Analysis*, 3rd ed., 675 pp., Chapman and Hall, Boca Raton, Fla.
Haslett, J., and A. Parnell (2008), A simple monotone process with application to radiocarbon-dated depth chronologies, *J. R. Stat. Soc., Ser. C*, *57*, 399–418.
Haslett, J., M. Whiley, S. Bhattacharya, M. Salter-Townsend, S. P. Wilson, J. R. M. Allen, B. Huntley, and F. J. G. Mitchell (2006), Bayesian palaeoclimate reconstruction, *J. R. Stat. Soc., Ser. A*, *169*(Part 3), 395–438.
Hertzberg, J. E., and M. W. Schmidt (2013), Refining *Globigerinoides ruber* Mg/Ca paleothermometry in the Atlantic Ocean, *Earth Planet. Sci. Lett.*, *383*, 123–133.
Hönisch, B., K. A. Allen, D. W. Lea, H. J. Spero, S. M. Eggins, J. Arbuszewski, P. DeMenocal, Y. Rosenthal, A. D. Russell, and H. Elderfield (2013), The influence of salinity on Mg/Ca in planktonic foraminifers—Evidence from cultured, core-top sediments and complementary δ^{18}O, *Geochim. Cosmochim. Acta*, *121*, 196–213.
Jackson, C. S., M. K. Sen, G. Huerta, Y. Deng, and K. P. Bowman (2008), Error reduction and convergence in climate prediction, *J. Clim.*, *21*(24), 6698–6709.
Jansen, E., et al. (2007), Paleoclimate, in *Climate change 2007: The Physical Science Basis. Contribution of Working Group I to the Fourth Assessment Report of the Intergovernmental Panel on Climate Change*, edited by S. Solomon, et al., pp. 433–497, Cambridge Univ. Press, Cambridge, U. K.
Key, R. M., A. Kozyr, C. Sabine, K. Lee, R. Wanninkhof, J. L. Bullister, R. A. Feely, F. J. Millero, C. Mordy, and T.-H. Peng (2004), A global ocean carbon climatology: Results from Global Data Analysis Project (GLODAP), *Global Biogeochem. Cycles*, *18*, GB4031, doi:10.1029/2004GB002247.
Kisakürek, B., A. Eisenhauer, F. Böhm, D. Garbe-Schönberg, and J. Erez (2008), Controls on shell Mg/Ca and Sr/Ca in cultured planktonic foraminiferan, *Globigeriniodes ruber* (white), *Earth Planet. Sci. Lett.*, *273*, 260–269.
Labeyrie, L., J. C. Duplessy, and P. L. Blanc (1987), Variations in mode of formation and temperature of oceanic deep waters over the past 125,000 years, *Nature*, *327*, 477–482.
Laepple, T., and P. Huybers (2013), Reconciling discrepancies between Uk37 and Mg/Ca reconstructions of Holocene marine temperature variability, *Earth Planet. Sci. Lett.*, *375*, 418–429.
Lea, D. W. (1999), Trace elements in foraminiferal calcite, in *Modern Foraminifera*, edited by B. K. Gupta, pp. 259–277, Kluwer Acad., U. K.
Lea, D. W., T. A. Mashiotta, and H. J. Spero (1999), Controls on magnesium and strontium uptake in planktonic foraminifera determined by live culturing, *Geochim. Cosmochim. Acta*, *63*(16), 2369–2379.
Lea, D. W., D. K. Pak, and H. J. Spero (2000), Climate impact of Late Quaternary equatorial Pacific sea surface temperature variations, *Science*, *289*(5485), 1719–1724.
LeGrande, A. N., and G. A. Schmidt (2006), Global gridded data set of the oxygen isotopic composition in seawater, *Geophys. Res. Lett.*, *33*, L12604, doi:10.1029/2006GL026011.
LeGrande, A. N., and G. A. Schmidt (2011), Water isotopologues as a quantitative paleosalinity proxy, *Paleoceanography*, *26*, PA3225, doi:10.1029/2010PA002043.
Lin, L., D. Khider, L. E. Lisiecki, and C. E. Lawrence (2014), Probabilistic sequence alignment of stratigraphic records, *Paleoceanography*, *29*, 976–989, doi:10.1002/2014PA002713.
Locarnini, R. A., A. V. Mishonov, J. I. Antonov, T. P. Boyer, and H. E. Garcia (2010), Volume 1: Temperature, in *World Ocean Atlas*, Ed. NOAA Atlas NESDIS 68, 184 pp., U.S. Gov. Print. Off., Washington, D. C.
Locarnini, R. A., et al. (2013), Volume 1: Temperature, in *World Ocean Atlas 2013, NOAA Atlas NESDIS 73*, edited by S. Levitus and A. V. Mishonov, 40. [Available at https://www.nodc.noaa.gov/OC5/woa13/pubwoa13.html.]
Marchitto, T. M., J. Lynch-Stieglitz, and S. R. Hemming (2005), Deep Pacific $CaCO_3$ compensation and glacial-interglacial atmospheric CO_2, *Earth Planet. Sci. Lett.*, *231*, 317–336.
Mathien-Blard, E., and F. Bassinot (2009), Salinity bias on the foraminifera Mg/Ca thermometry: correction procedure and implications for past ocean hydrographic reconstructions, *Geochem. Geophys. Geosyst.*, *10*, Q12011, doi:10.1029/2008GC002353.
Mix, A. C., and W. F. Ruddiman (1984), Oxygen-isotope analyses and Pleistocene ice volumes, *Quat. Res.*, *21*, 1–20.

Mohtadi, M., S. Steinke, J. Groeneveld, H. G. Fink, T. Rixen, D. Hebbeln, B. Donner, and B. Herunadi (2009), Low-latitude control on seasonal and interannual changes in planktonic foraminiferal flux and shell geochemistry off south Java: A sediment trap study, *Paleoceanography*, *24*, PA1201, doi:10.1029/2008PA001636.

Mohtadi, M., D. Oppo, A. Luckge, R. DePol-Holz, S. Steinke, J. Groeneveld, N. Hemme, and D. Hebbeln (2011), Reconstructing the thermal structure of the upper ocean: insights from planktic foraminifera shell chemistry and alkenones in modern sediments of the tropical eastern Indian Ocean, *Paleoceanography*, *26*, PA3219, doi:10.1029/2011PA002132.

Nouet, J., and F. Bassinot (2007), Dissolution effects on the crystallography and Mg/Ca content of planktonic foraminifera *Globorotalia tumida* (Rotaliina) revealed by X-ray diffractometry, *Geochem. Geophys. Geosyst.*, *8*, Q10007, doi:10.1029/2007GC001647.

Nürnberg, D., J. Bijma, and C. Hemleben (1996), Assessing the reliability of magnesium in foraminiferal calcite as a proxy for water mass temperatures, *Geochim. Cosmochim. Acta*, *60*(5), 803–814.

Parnell, A., J. Sweeney, T. K. Doan, M. Salter-Townsend, J. R. M. Allen, B. Huntley, and J. Haslett (2014), Bayesian inference for paleoclimate with time uncertainty and stochastic volatility, *J. R. Stat. Soc. Ser. C*, *64*(1), 115–138.

Regenberg, M., D. Nurnberg, S. Steph, J. Groeneveld, D. Garbe-Schonberg, R. Tiedemann, and W.-C. Dullo (2006), Assessing the effect of dissolution on planktonic foraminiferal Mg/Ca ratios: Evidence from Caribbean core tops, *Geochem. Geophys. Geosyst.*, *7*, Q07P15, doi:10.1029/2005GC001019.

Regenberg, M., A. Regenberg, D. Garbe-Schonberg, and D. W. Lea (2014), Global dissolution effects on planktonic foraminiferal Mg/Ca ratios controlled by the calcite-saturation state of bottom waters, *Paleoceanography*, *29*, 127–142, doi:10.1002/2013PA002492.

Richey, J. N., R. Z. Poore, B. P. Flower, and D. J. Hollander (2012), Ecological controls on the shell geochemistry of pink and white *Globigerinoides ruber* in the northern Gulf of Mexico: Implications for paleoceanographic reconstructions, *Mar. Micropaleontol.*, *82-83*, 28–37.

Rosenthal, Y., and G. P. Lohmann (2002), Accurate estimation of sea surface temperatures using dissolution-corrected calibrations for Mg/Ca paleothermometry, *Paleoceanography*, *17*(3), 1044, doi:10.1029/2001PA000749.

Rosenthal, Y., et al. (2004), Interlaboratory comparison study of Mg/Ca and Sr/Ca measurements in planktonic foraminifera for paleoceanographic research, Geochemistry, Geophysics, *Geosystems*, *5*, Q04D09, doi:10.1029/2003GC000650.

Russell, A. D., B. Hönisch, H. J. Spero, and D. W. Lea (2004), Effects of seawater carbonate ion concentration and temperature on shell U, Mg, and Sr in cultured planktonic foraminifera, *Geochim. Cosmochim. Acta*, *68*(21), 4347–4361.

Sabbatini, A., F. Bassinot, S. Boussetta, A. Negri, H. Rebaubier, F. Dewilde, J. Nouet, N. Caillon, and C. Morigi (2011), Further constraints on the diagenetic influences and salinity effect on *Globigerinoides ruber* (white) Mg/Ca thermometry: Implications in the Mediterranean Sea, *Geochem. Geophys. Geosyst. 12*, Q10005, doi:10.1029/2011GC003675.

Sadekov, A. Y., S. M. Eggins, P. De Dekker, U. S. Ninnemann, W. Kuhnt, and F. Bassinot (2009), Surface and sub-surface seawater temperature reconstruction using Mg/Ca microanalysis of planktonic foraminifera *Globigerinoides ruber*, *Globigerinoides sacculifer* and *Pulleniatina obliquiloculata*, *Paleoceanography*, *24*, PA3201, doi:10.1029/2008PA001664.

Schrag, D. P., G. Hampt, and M. D.W. (1996), Pore fluid constraints on the temperature and oxygen isotopic composition of the glacial ocean, *Science*, *272*, 1930–1932.

Shackleton, N. J. (1974), Attainment of isotopic equilibrium between ocean water and benthonic foraminifera genus *Uvigerina*: Isotopic changes in the ocean during the last glacial, in *Les méthodes quantitatives d'étude des variations du climat au cours du Pleistocène*, edited by centre national de la recherche scientifique (CNRS), pp. 203–209, Cent. Natl. de la Rech.Sci., Gif-sur-Yvette, France.

Stott, L., C. Poulsen, S. Lund, and R. Thunell (2002), Super ENSO and global climate oscillations at millennial time scales, *Science*, *297*(5579), 222–226.

Stott, L., A. Timmermman, and R. Thunell (2007), Southern hemisphere and deep-sea warming led to deglacial atmospheric CO_2 rise and tropical warming, *Science*, *318*, 435–438.

Sueyoshi, T., et al. (2013), Set-up of the PMIP3 paleoclimate experiments conducted using an Earth system model, MIROC-ESM, *Geosci. Model Dev.*, *6*, 819–836.

Tebaldi, C., R. O. Smith, D. Nychka, and L. Mearns (2005), Quantifying uncertainty in projections of regional climate change: a Bayesian approach to the analysis of multimodel ensembles, *J. Clim.*, *18*, 1524–1540.

Tierney, J. E., and M. P. Tingley (2014), A Bayesian, spatially-varying calibration model for the TEX86 proxy, *Geochim. Cosmochim. Acta*, *127*, 83–106.

Tingley, M. P., and P. Huybers (2010), A Bayesian algorithm for reconstructing climate anomalies in space and time. Part I: Development and applications to paleoclimate reconstruction problems, *J. Clim.*, *23*(10), 2759–2781.

van Hueven, S., D. Pierrot, E. Lewis, and W. R. Wallace (2009), *MATLAB Program Developed for CO_2 System Calculations*, Oak Ridge National Laboratory, Oak Ridge, Tenn.

Waelbroeck, C., L. Labeyrie, E. Michel, J. C. Duplessy, J. F. McManus, K. Lambeck, E. Balbon, and M. Labracherie (2002), Sea level and deep water temperature changes derived from benthic foraminifera isotopic records, *Quat. Sci. Rev.*, *21*, 295–305.

Xu, J., W. Kuhnt, A. Holbourn, M. Regenberg, and N. Andersen (2010), Indo-Pacific warm pool variability during the Holocene and Last Glacial Maximum, *Paleoceanography*, *25*, PA4230, doi:10.1029/2010PA001934.

Yu, J., W. S. Broecker, H. Elderfield, Z. Jin, J. McManus, and F. Zhang (2010), Loss of carbon from the deep sea since the last glacial maximum, *Science*, *330*, 1084–1087.

Zweng, M. M., et al. (2013), Volume 2: Salinity, in *World Ocean Atlas 2013, NOAA Atlas NESDIS 74*, edited by S. Levitus and A. V. Mishonov, 39. [Available at https://www.nodc.noaa.gov/OC5/woa13/pubwoa13.html.]